Shear, Strain, and Richardson Number Variations in the Thermocline. Part II: Modeling Mixing

ROBERT PINKEL

Marine Physical Laboratory, Scripps Institution of Oceanography, La Jolla, California

STEVEN ANDERSON

Woods Hole Oceanographic Institution, Woods Hole, Massachusetts

(Manuscript received 14 December 1994, in final form 18 June 1996)

ABSTRACT

Gregg has provided observational evidence that averaged estimates of dissipation, ϵ, vary approximately as the square of the internal wave field energy level $\epsilon \sim E^2$. He notes that the finding is consistent with a specific model for energy transfer in the internal wave field proposed by Henyey et al. If it is also consistent with a purely statistical breaking model, based on the random superposition of independent waves, support for any particular dynamic scenario vanishes.

However, most previous statistical models of the wave breaking process have demonstrated an extreme sensitivity of dissipation to energy level. Doubling E results in an increase of dissipation by a factor of 2×10^5 in the early model of Garrett and Munk and by 10^3 in the later model of Desaubies and Smith.

These mixing models are revisited, attempting to reconcile their predictions with the observations of Gregg. An extensive Doppler sonar (5.5-m vertical resolution) and CTD (5400 profiles to 420 m) dataset, obtained from the Research Platform *FLIP* during the SWAPP experiment, is applied to the problem. A model for the probability density function (pdf) of Richardson number is developed (Part I of this work), accounting for both shear and strain variability. This pdf is an explicit function of the vertical differencing scale, $\overline{\Delta z}$, over which shear and strain are estimated. From this pdf, a related probability density of overturning can be derived as a function of overturn scale and internal wave field energy level. The third moment of this pdf is proportional to the buoyancy flux, which can be related to dissipation, assuming a fixed flux Richardson number.

When this finite difference approach is pursued, dissipation levels are found to vary nearly as E^2 for a variety of contrasting internal wave spectral models. Gregg's constant of proportionality is recovered, provided independent realizations of the Richardson number process are said to occur every 10–14 hours.

1. Introduction

It is presently thought that mechanical mixing events in the ocean interior account for 5%–10% of the mean buoyancy flux required to maintain the deep oceans in a steady state (e.g., Munk 1966; Gregg 1989). The fine-scale internal wave field is a probable energy source for these events. Typical overturn scales are of order 1 m. Presumably, the wave field is forced by yet larger scale phenomena. The interactions that occur at each stage of this process are presently being explored.

Gregg (1989) has presented data suggesting a linkage between highly averaged estimates of finescale shear variance and corresponding averages of mechanical dissipation ϵ. Gregg's relationship, expressed in terms of an eddy diffusivity, A_ρ m^2 s^{-1}, is

$$A_\rho \leq 5 \times 10^{-6} \langle S_{10}^2 \rangle^2 / \langle S_{GM}^2 \rangle^2 \quad (1)$$

(Gregg and Kunze 1991).

The 10-m shear variance $\langle S_{10}^2 \rangle$ is used by Gregg as an indicator of the overall level of energy in the internal wavefield, relative to a canonical level $\langle S_{GM}^2 \rangle$. He does not suggest that S_{10} is directly involved in generating the observed dissipation in the thermocline. Rather, the Garrett–Munk spectral model (Garrett and Munk 1972a, 1975; Cairns and Williams 1976) is used to infer smaller-scale wave statistics from his 10-m observations.

Gregg's observation, $A_\rho \propto \langle S_{10}^2 \rangle^2$, is consistent with the dynamical model of Henyey et al. (1986, hereafter H86), which provides an explicit mechanism for ocean mixing. The vertical propagation of small-scale, slowly moving, internal wave packets is perturbed by the passage of faster propagating large-scale waves. While the details of this perturbation depend on the geometry of the individual encounter, there is a net tendency for the vertical scale of the short wave to be reduced further. Henyey et al. (1986), set a vertical scale of 5 m as an effective wave breaking threshold. They track the trans-

Corresponding author address: Dr. Robert Pinkel, Marine Physical Laboratory, Scripps Institution of Oceanography, University of California, San Diego, La Jolla, CA 92093-0213.
E-mail: RPINKEL@UCSD.EDU

fer of wave energy across this threshold and equate it to an effective mean turbulent dissipation rate. The general success of the Gregg (1989) relationship has been cited by some (e.g. Polzin, 1992) as evidence that the H86 scenario indeed describes the dominant mixing process in the open ocean thermocline. A variety of interesting dynamical consequences and constraints follow.

On the other hand, if the simple random superposition of shear and strain (N^2) fluctuations also leads to mixing consistent with Gregg (1989), the need to invoke a specific dynamic scenario vanishes. Purely statistical mixing models have been offered by Bretherton (1969, hereafter B69), Garrett and Munk (1972b, hereafter GM72b), Munk (1981, hereafter M81), and Desaubies and Smith (1982, hereafter DS82). All studies except M81 found modeled mixing rates to be extremely sensitive to overall internal wave energy levels. In the GM72b model, doubling the internal wave energy increased the predicted dissipation by a factor of 1.9×10^5. In DS82, buoyancy fluxes increased by three orders of magnitude when mean wavefield energy levels were doubled.

Since these early modeling efforts, Pinkel et al. (1991), Anderson (1992), Polzin (1992), Pinkel and Anderson (1992, hereafter PA92), and Gregg et al. (1993) have examined shear, strain, and dissipation statistics in some detail. Squared shear, $S^2 = (\partial u/\partial z)^2 + (\partial v/\partial z)^2$, is clearly better modeled as a χ^2 variable with two degrees of freedom (as in DS82) than as a Gaussian variable (B69, GM72b, M81). Väisälä frequency variability is well modeled by the gamma (Erlang) probability distribution (PA92).

Using these contemporary probability distributions, it is of interest to see whether a classical mixing model can be reconciled with the Gregg (1989) result. The present work differs from previous efforts in that it is not tied to a specific internal wave spectral model. Also, it is based on the notion of a ''finite difference'' Richardson number, where shear and strain are defined as differences over a specified vertical interval. As a direct consequence of this definition, we can investigate whether multiple small overturns, ''puffs,'' or the rare large ''big bangs'' are the dominant contributors to mixing. Does this situation change with changing wavefield energy level?

The modeling effort is supported by observations of shear and strain that are quasi continuous in time and depth. The data are obtained using a 160-kHz Doppler sonar and a repeatedly profiling CTD (Anderson 1992) mounted on the Research Platform *FLIP*. Approximately 5400 CTD profiles, obtained in the early stages of the 1990 experiment SWAPP, are applied to this study. The reader is referred to Part I of this work (Pinkel and Anderson 1997, hereafter PA97) for a description of the data.

2. Modeling mixing

We start with the problem as idealized by GM72b. The model is based in the shear instability mechanism of Miles (1961) and Howard (1961). The Richardson number, $\mathrm{Ri} = N^2/S^2$, where N is the buoyancy frequency, is assumed to completely govern the occurrence of mixing events. In a given realization of a vertical profile of N^2, S^2, regions of $\mathrm{Ri} < 0.25$ are identified as mixing sites. The sites are assumed to be mixed to a uniform density over their vertical extent.[1] The change in potential energy associated with this idealized process can be converted to a buoyancy flux, provided a critical timescale, T, related to the time between independent realizations of this process, is introduced.

Central to the one-dimensional mixing model is the probability density of overturning $Q(\Delta)$, where $Q(\Delta)d\Delta$ gives the probability of occurrence of an overturn of vertical scale between Δ and $\Delta + d\Delta$ per unit depth per unit time (GM72b). The change in potential energy per unit area associated with perfect mixing over height Δ is (following GM72b)

$$E_\rho(\Delta) = \frac{1}{12}\rho N^2 \Delta^3. \tag{2}$$

The average change in potential energy per unit time per unit volume is

$$F_\rho = \int_0^\infty E_\rho(\Delta) Q(\Delta)\, d\Delta. \tag{3}$$

Modeling this buoyancy flux in terms of an eddy diffusivity,

$$F_\rho = A_\rho\, g\, \partial\rho/\partial z = \rho A_\rho N^2, \tag{4}$$

implies

$$A_\rho = \frac{1}{12}\int_0^\infty \Delta^3 Q(\Delta)\, d\Delta. \tag{5}$$

The challenge for this class of mixing models is to produce a realistic $Q(\Delta)$. In their previous effort, GM72b invoke Rice statistics appropriate to Gaussian S^2 fluctuations to estimate the density of critical events in depth and time. DS82 simulate Richardson number profiles numerically in an effort to quantify the incidence of critical events per unit depth. These studies exhibited an extreme sensitivity of the inferred mixing rates to energy level, in contrast to Gregg's (1989) more recent observation.

In revisiting this problem, Munk (1981) associates instability with the probability that $\phi > 1$, where ϕ is a scalar related to $(S^2/\overline{N^2})^{1/2}$, which is presumed to have Gaussian statistics. The extreme sensitivity of previous efforts is replaced with a more moderate dependence of

[1] GM72b chose to mix the fluid over a vertical extent slightly larger than the initial $\mathrm{Ri} < 1/4$ region. We neglect this refinement here, in the interest of simplicity.

dissipation on wavefield energy.[2] However, the Gaussian breaking criterion is problematic, given the clearly non-Gaussian nature of the Richardson number pdfs presented in PA97.

With newer pdfs, supported by observations, we attempt a more realistic model of $Q(\Delta)$. The modeling effort is simplified in that the pdfs presented in PA97 are explicit functions of the vertical differencing scale $\overline{\Delta z}$. We apply the Eulerian model pdf for Richardson number, derived under the hypothesis that cross-isopycnal differences in horizontal velocity $(\Delta u)^2$ are independent of strain (PA97, Table I, Eulerian II). The reasonable alternative hypothesis that cross-isopycnal shear is independent of strain was not supported by the observations.

We start by integrating the pdf of inverse Richardson number to form a cumulative distribution function:

$$C_{E\text{II}}(R^{-1}|\overline{\Delta z}) = 1 - (1 + R^{-1}/\kappa)^{-(\kappa+1)}. \quad (6)$$

Here $R \equiv \text{Ri}/\text{Ri}^*$ where $\text{Ri}^* \equiv \overline{N^2}\ \overline{\Delta z}^2/\langle \Delta u^2 \rangle$, and $\kappa = \kappa_0 \overline{\Delta z}$, where κ_0 is a constant set by the strain spectral level. The subscript E refers to a statistic accumulated in an Eulerian frame.

Instability over vertical scale Δ occurs when $\text{Ri}^{-1} > 4$, or $R^{-1} > 4\text{Ri}^*$. Thus, the relative probability of instability is

$$B(\Delta) = 1 - \text{C}(4\text{Ri}^*|\Delta) \quad (7a)$$

$$B_{E\text{II}}(\Delta) = (1 + 4\ \text{Ri}^*/\kappa)^{-(\kappa+1)}. \quad (7b)$$

This breaking probability is derived from a finite difference over Δ meters. It is shown in the appendix that the function

$$\hat{\hat{Q}}(\Delta) = -\frac{1}{\Delta}\frac{dB(\Delta)}{d\Delta} \qquad \Delta > 0 \quad (8)$$

gives the probability density of critical Ri over vertical scale Δ. Here $\hat{\hat{Q}}$ is not quite a proper pdf in that its integral over all Δ is less than unity. Most of the time, the ocean is not overturning at any scale. We define a ''nonevent'' as an overturn of height $\Delta = 0$ and use the Dirac delta to specify

$$\hat{Q}(\Delta) = q_o\delta(\Delta) + \hat{\hat{Q}}(\Delta), \quad (9)$$

where q_0 is chosen such that the integral of $\hat{Q}$ over $(0 \le \Delta < \infty)$ is unity.

The function $\hat{Q}$ so derived has units of probability of critical Richardson number per unit Δ per unit depth per realization of the process. It falls short of the GM72b specification in that there is no sense of time evolution, the number of independent critical events per unit time. Following GM72b, we introduce a characteristic mixing time T, here the time per realization, such that

$$A_\rho = \frac{1}{12T}\int_0^\infty \Delta^3\hat{Q}(\Delta)\, d\Delta. \quad (10)$$

Using the GM72a spectral model, GM72b suggest

$$T_{\text{GM}} = \pi\,(Nf)^{-1/2}, \quad (11)$$

where f is the local inertial frequency. At 30° latitude, N = 3cph, $T_{\text{GM}} = 1.41$ h.

Here we will maintain T as an independent time parameter, isolating its influence from the many other factors that affect the eddy diffusivity estimate.

With this formalism in place, it remains to evaluate expressions (8)–(10) and estimate mean mixing rates. The interesting variability is governed by the behavior of $\text{Ri}^*(\overline{\Delta z})$:

$$Ri^*(\Delta z) = \overline{N^2}\cdot\left(\int_0^\infty E(k)\text{sinc}^2\left(\frac{k\Delta z}{2\pi}\right) dk\right)^{-1}. \quad (12)$$

Here $E(k)$ is the one-sided vertical wavenumber spectrum of shear. Previous modeling efforts have relied on the Garrett–Munk internal wave model (Garrett and Munk 1972a, 1975; M81). In their pioneering effort, GM72b assume the form of the spectrum to be independent of energy level (Fig. 1a). More recently, inspired by the oceanic observations of Duda and Cox (1989), as well as atmospheric observations, Muller et al. (1991) suggest a revised spectrum with a limiting high wavenumber form (Fig. 1b). The Muller et al. spectrum is identical to the GM spectrum at the canonical GM energy level. PA92 conjecture a yet more extreme spectral behavior for strain fluctuations. In their idealized model, the spectral bandwidth is inversely proportional to energy level. If the shear spectrum varied similarly one would have the family of spectra seen in Fig. 1c.

Differences in the form of the three spectral models are manifest in the behavior of the associated Ri* (Figs. 1d–f). The GM model results in a set of congruent curves, changing only by a constant factor with spectral level. The other spectral models yield more complex behavior. Since their effective spectral bandwidth decreases with increasing energy, the dependence of Ri* on separation becomes stronger with increasing energy.

---

[2] In GM72b, the probability of a breaking event per realization varies as $\exp(-2N^2/\langle S^2\rangle) \approx \exp(-16.2N_0/N(z))$, where N_0 is the scale Väisälä frequency, taken as 3 cph. At a depth such that $N(z) = N_0$, doubling the shear variance increases the probability of breaking by the factor $\exp(8.1) = 2.9 \times 10^3$. In Munk (1981), the analogous breaking probability is given by

$$(2\langle S^2\rangle/\overline{N^2})^{1/2}\exp(-\overline{N^2}/2\langle S^2\rangle) \approx (2 \times 1.72)^{1/2}\exp[-1/(2 \times 1.72)].$$

[q2] The form of this expression has changed only slightly from the 1972 version. However, the expected shear variance in the GM spectral model was increased by a factor of 10 (*at* $N(z) = N_0$) or more ($N(z) < N_0$) between 1972 and 1981. Thus, the probability of observing a critical event at the canonical GM energy level is no longer $\sim e^{-16.2}$, but now $e^{-.29}$. A doubling of shear variance produces an increase of only $e^{.145} = 1.15$ in this second exponential. The 1981 breaking model thus appears much less sensitive to variations in energy level than the 1972 model. This is primarily due to the increase in shear variance in the internal wave spectral model, rather than a fundamental change in the mixing model.

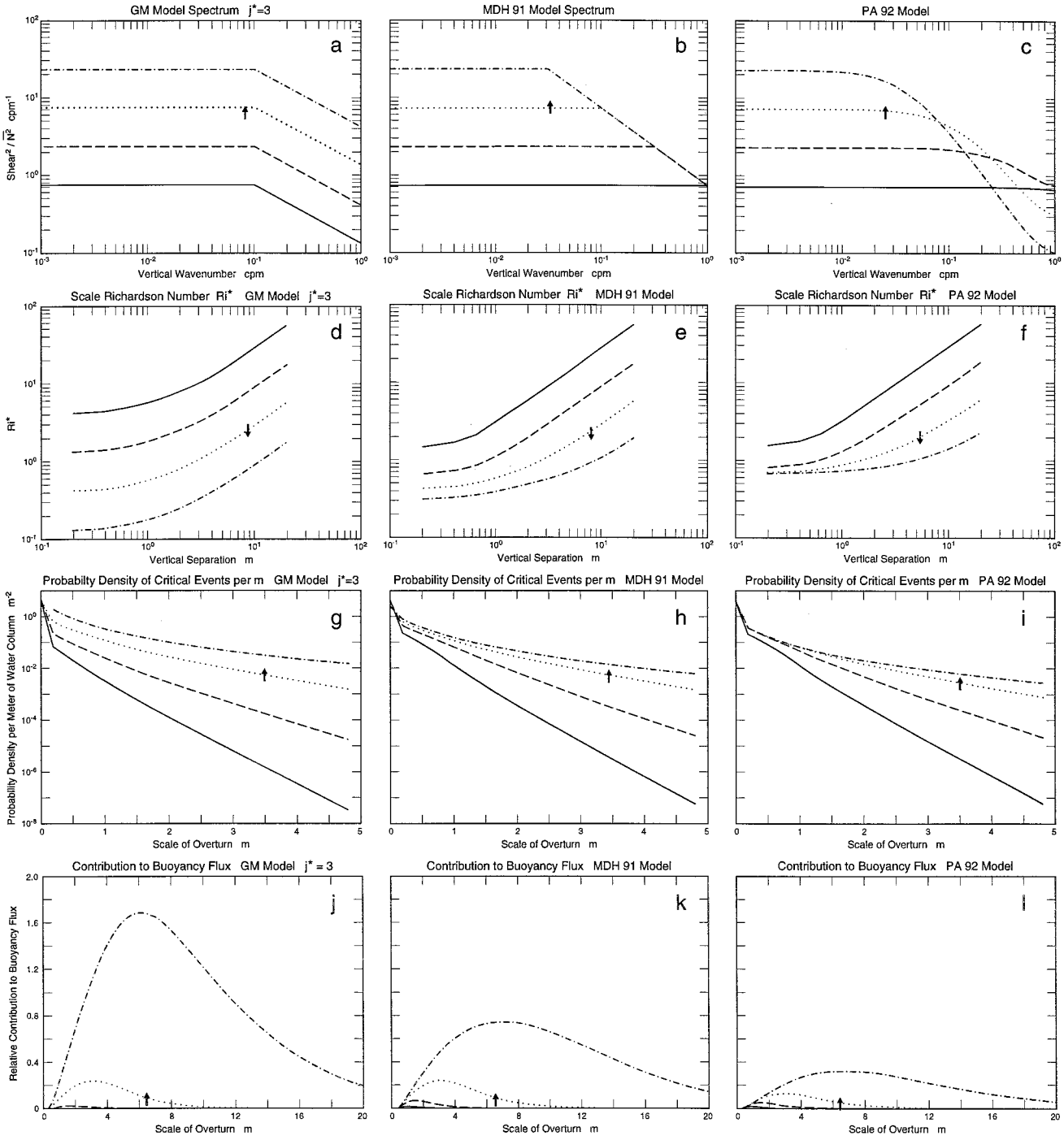

FIG. 1. Schematic model spectra of shear as a function of vertical wavenumber at four energy levels. The models presented are by (a) Garrett and Munk, (b) Muller et al., and (c) Pinkel and Anderson. The arrow in each plot indicates the canonical GM76 energy level. The associated functions $\mathrm{Ri}^*(\overline{\Delta z})$ for the three models (d, e, f). Resulting models for the pdf of instability, $Q(\Delta)$ (g, h, i) and the relative contribution to the buoyancy flux $\Delta^3 Q(\Delta)$ (j, k, l). Note that the vertical scale of the dominant contributor to the buoyancy flux increases with increasing wavefield energy.

This variation in behavior with spectral level strongly influences the mixing prediction.

The indicated behavior of Ri* at separations $\Delta z \leq 1$ m is an artifact of the spectral models, which all assume that there is zero shear variance at scales smaller than 1 m. Field observations, in fact, show strong spectral variability in this region (e.g., Gargett et al. 1981), although this variance is not thought to be associated with reversible fine structure.

The model probability density functions $\hat{Q}(\Delta)$, pre-

sented in Figs. 1g–i, show nearly exponential form for $\Delta > 1$ m. The discontinuity at zero scale reflects the probability of ''no overturn'' occurring. The magnitude of the discontinuity decreases as energy levels increase.

Plots of $\Delta^3 Q(\Delta)$ (Figs. 1j–l) illustrate graphically the rapid increase in overturning with increasing energy associated with the GM model (j) relative to the progressive bandwidth models (k, l). All models exhibit an increase in the *scale* of the dominant contributor to the buoyancy flux with increasing energy. Rare ~3 m events are predicted to be the dominant contributor to mixing in a GM wave field at the canonical GM75 energy level (j). With the alternative spectral models (k, l) slightly smaller overturns are the dominant contributors. All predictions are in general accord with observations (e.g., Evans 1982) and the modeling effort of DS82.

The modeled mixing results are summarized in Figs. 2a,b. Here the effective diffusivity in ''m^2 per realization'' is plotted as a function of the spectral level of the normalized shear spectrum (a) and the 10-m scale Richardson number (b). The inverse of Ri*(10) is nearly equivalent to Gregg's (1989) 10-m shear measurement. (When considering spectral models whose form evolves with energy level, the 10-m shear variance and the spectral energy level are slightly different.)

The diffusivities can be converted to physical units, $m^2\ s^{-1}$, through the characteristic timescale T, the time between independent realizations of the Richardson number field. Using $T_{GM} = 1.41$ h as a reference value, the Gregg (1989) recipe [Eq. (1)] is converted to the present units and plotted in Figs. 2a,b for reference.

3. Discussion

The diffusivity as a function of spectral level based on the PA92 spectrum exhibits similar slope to the Gregg (1989) model, but is a factor of 8–10 greater. The Muller et al. (1991) diffusivity is of slightly steeper slope, again a factor of 10 larger than Gregg's diffusivity. These estimates could be easily reconciled with Gregg's prediction by assuming T = 10–14 h, as opposed to the 1.4 h used here. Perhaps not coincidentally, Briscoe (1977), in his study of internal wave statistics, suggested a timescale of 11 h for independent measurements of shear, based on midlatitude observations (28°N). The GM diffusivity has a much steeper slope, varying as E^{3-4}, rather than the E^2 predicted by Gregg. All models predict a curious decrease in slope at high wavefield energy levels. For the PA92 and Muller et al. (1991) models, diffusivities appear to level off at spectral energy levels 8–10 times the GM standard.

These predictions reflect the interplay of the specific Ri probability model and the three spectral models in the finite difference formalism presented above. It is of value to test the sensitivity of these predictions to the various assumptions involved. A major assumption is that the strain spectrum varies as described in PA92. As the spectral level is increased, spectral bandwidth decreases, as indicated for shear in Fig. 1c. The observational evidence for this behavior is sketchy, as is the evidence that shear and strain spectral levels rise and fall in tandem.

In Figs. 3a,b we repeat the diffusivity calculations, this time holding the strain spectral level fixed ($\kappa_0 = 1.2$). The PA92 and Muller et al. (1991) predictions again are a factor of 8–10 greater than Gregg (1989). The GM diffusivity maintains its relatively steep slope. With the strain spectrum fixed, the diffusivities increase monotonically with wavefield energy, in contrast to the previous case. A careful study of the covariance of the shear and strain fields is clearly warranted.

As a second sensitivity study, we examine the effects of neglecting strain variability entirely. Probability density functions of inverse Richardson number based on shear fluctuations alone were presented by Gregg et al. (1993). PA97 term this the ''traditional model'' of the inverse Richardson number. The associated probability density function for Ri^{-1} is exponential. Based on this simple model, diffusivities are recalculated and presented in Figs. 3c,d. The predictions associated with the PA92 and Muller et al. (1991) spectral models again nearly parallel the Gregg observation, now with very little offset. The GM spectrum also provides a result consistent with Gregg (1989), at and above the canonical GM energy level. This replicates the M81 finding. At low shear variance levels, the slope of the relationship greatly steepens, reminiscent of the extreme sensitivity seen in GM72b.

Several concerns remain associated with the modeling process. Specifically, the gamma model strain pdfs used in the derivation of the Richardson number pdf are thought to be inappropriate at vertical scales smaller than 3 m (PA92). Given the increasing importance of strain with decreasing scale, this is a significant issue.

It has been assumed, for simplicity, that the existence of critical Ri over height Δ implies perfect mixing over that height alone, with no ''entrainment mixing'' over a larger regime, either vertically or laterally. This is a clear idealization that calls for refinement.

PA97a (Fig. 7) suggests that Ri*(Δz) does not vary significantly with depth. Thus, any significant depth dependence in this mixing model is introduced by the timescale T. Using T_{GM}, we find $A_\rho \sim N^{1/2}$, in conflict with Gregg's observations. (We also find that A_ρ vanishes on the equator!) Clearly, the time evolution of the Richardson number must be considered explicitly when forming more accurate models of the mixing process.

In summary, a statistical model for the probability density of Richardson number has been developed (PA97) and applied to the problem of mixing in the ocean thermocline. The finite difference formalism used in its derivation enables a straightforward interpretation in terms of $Q(\Delta)$, a probability density of instability as a function of the height of instability, per unit depth, per realization. It is found that size of the dominant

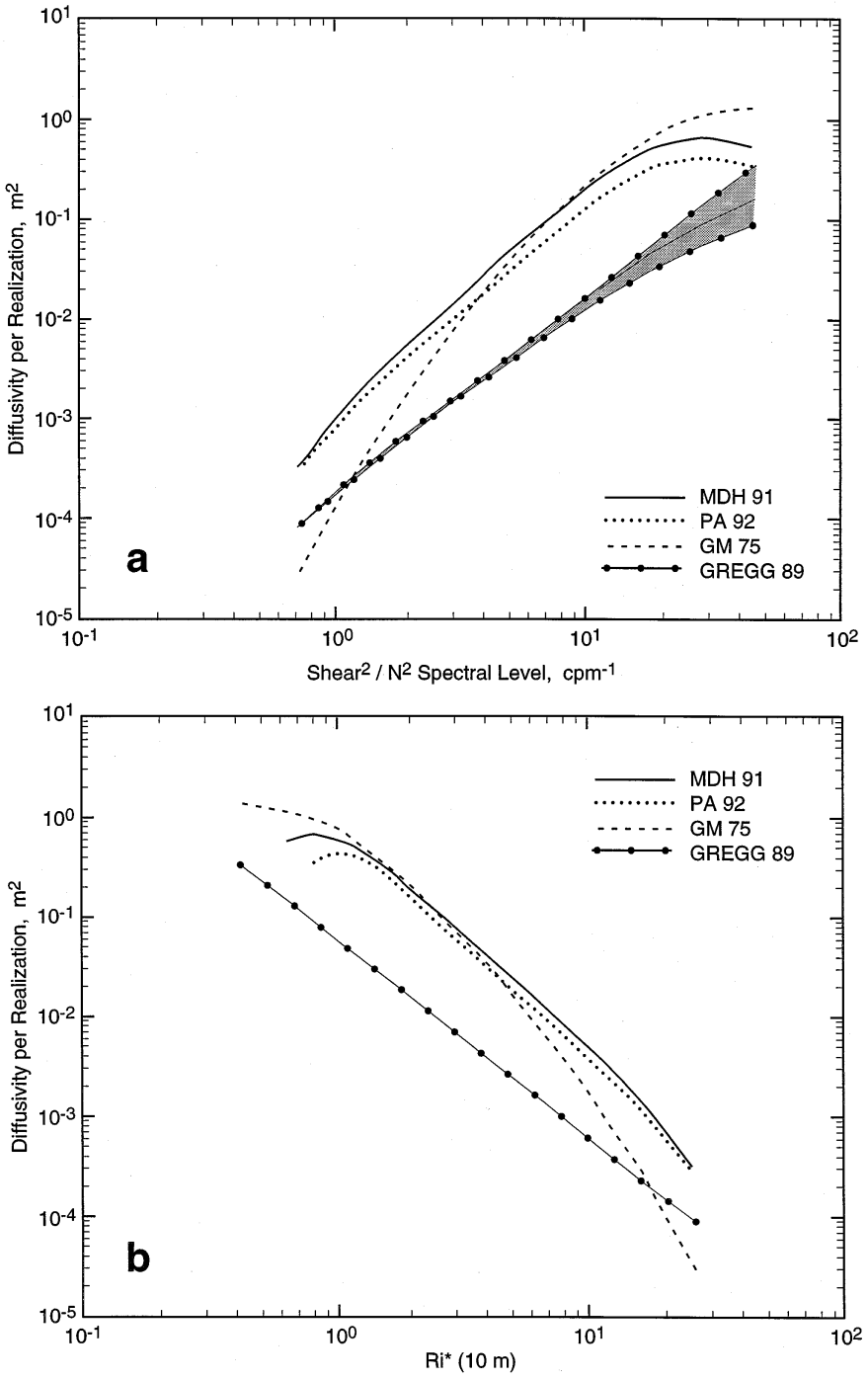

FIG. 2. The effective eddy diffusivity per realization of the process, plotted as a function of (a) spectral level and (b) 10-m scale Richardson number. The Gregg (1989) synthesis of ocean observations is plotted for comparison. Results can be converted to an effective diffusivity through division by a characteristic timescale T. The GM72b timescale $T_{GM} = \pi(fN)^{-1/2} = 1.41$ h is used to convert Gregg's result to this format. Increasing this timescale would result in close agreement between the PA92 model, the Muller et al. model, and Gregg's observations.

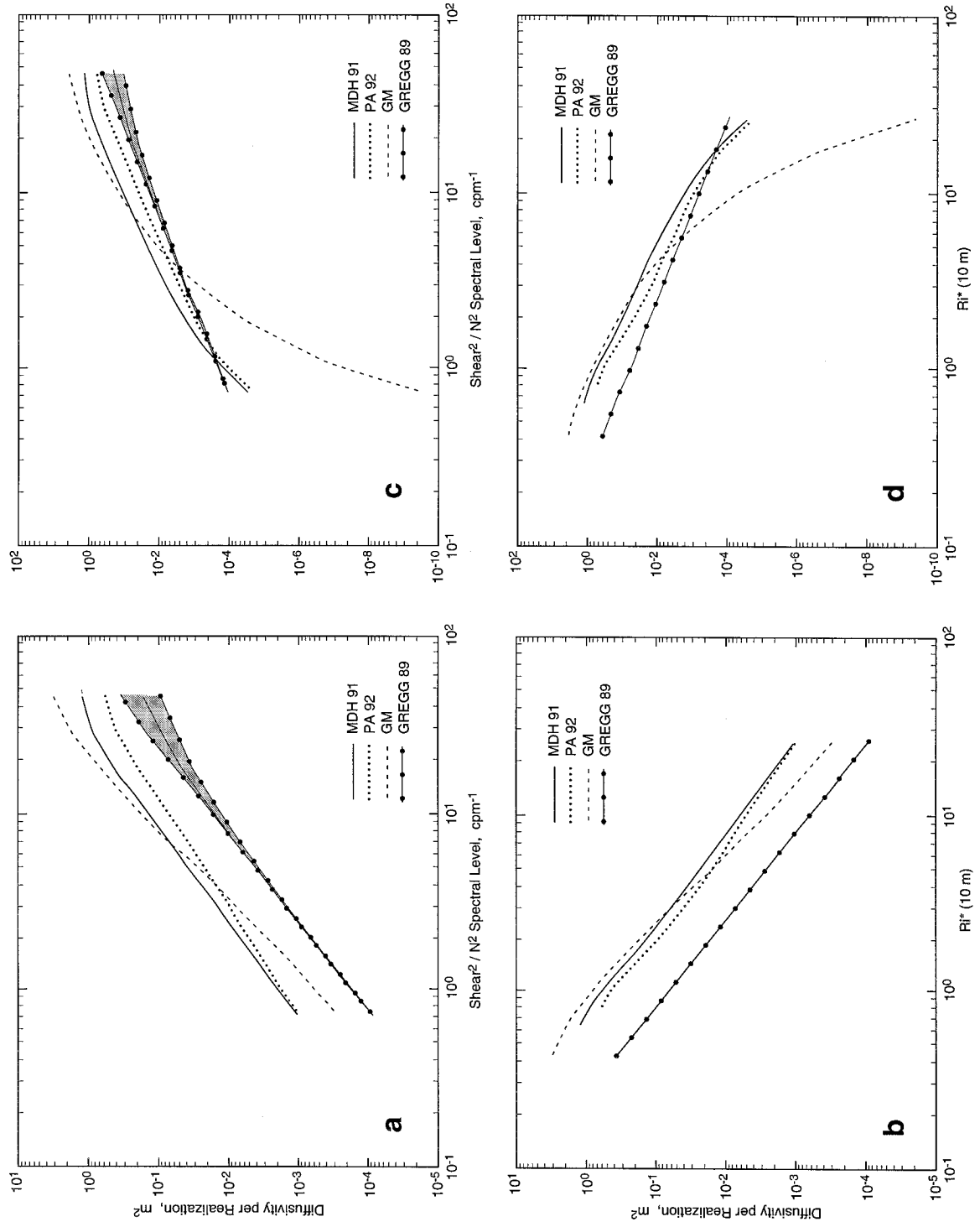

FIG. 3. (a,b) Eddy diffusivity calculations as in Fig. 2, with shear spectral variability maintained and the strain spectrum held fixed at typical open ocean levels ($\kappa_0 = 1.2$ m^{-1}). With the strain spectral bandwidth fixed, the dependence of A_ρ on Ri* (or alternatively $\langle S^2 \rangle$) is maintained even at high energy levels. (c,d) The eddy diffusivity, as estimated from a model that neglects strain variation entirely. Diffusivities are reduced a factor of ~2, (high energy) to 5 (low energy) for the progressive bandwidth spectral models. For the Garrett–Munk spectrum, the diffusivity is highly dependent on Ri* at low Ri*, becoming more consistent with Gregg (1989) at higher energy levels.

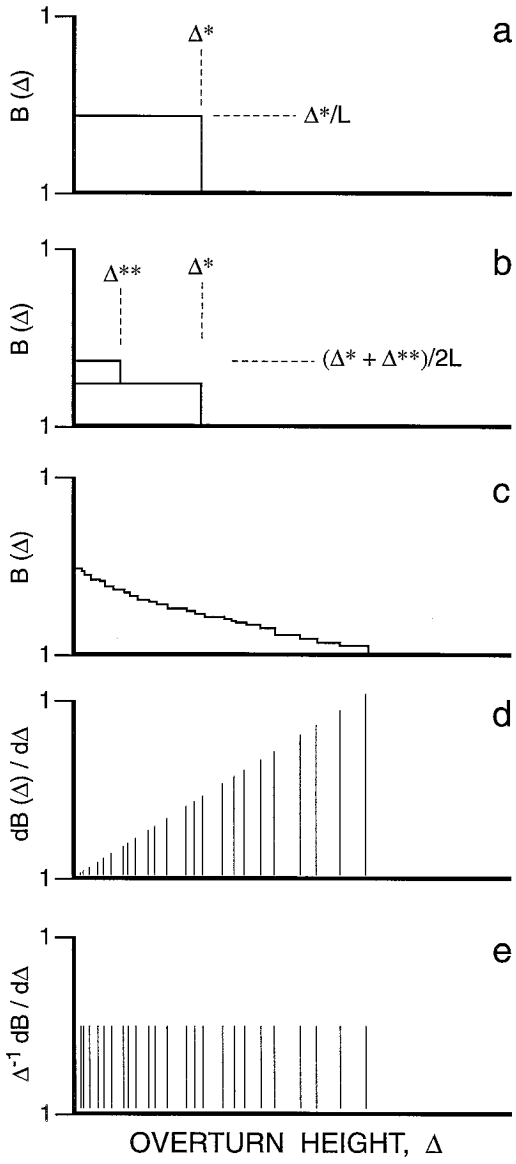

FIG. 4. (a) The sample probability of instability over scale Δ, as inferred from a vertical profile of length L m, in which a single instability of height Δ* m is encountered. (b) The sample probability after two profiles, the second detecting an unstable region of height Δ**. (c) Following many profiles, the sample probability function approaches a smooth form. (d) Differentiating the sample probability function reveals a comb of Dirac delta functions, with one corresponding to each observed instability. The magnitude of the delta function is proportional to the size of the instability. (e) Normalized by instability size, a uniform comb of delta functions is recovered. This can be integrated over fixed Δ bins to approximate the process pdf, $Q(\Delta)$.

contributor to the buoyancy flux increases with increasing wavefield energy. The details of this evolution depend on the specific internal wave spectral model being considered.

Eddy diffusivity predictions are created based on three shear spectral models. The progressive bandwidth models suggested by Muller et al. (1991) and PA92 produce diffusivities in excellent accord with the Gregg (1989) observational synthesis, provided a characteristic time, T, between independent realizations is set at 10–14 h. Diffusivity estimates based on changing the level of the GM75 shear spectrum while maintaining its bandwidth exhibit greater sensitivity to spectral levels than Gregg has observed. This purely statistical model calls for a time scale whose variation with depth, latitude, and wavefield energy level requires dynamical explanation. The 1-d model is blind to the important issue of the lateral extent of low Ri regions and mixing patches. On the other hand, since much of the Gregg (1989) result can be explained by the random superposition of shear and strain fields, consistency with his observations does not necessarily confirm the validity of any particular dynamic scenario.

Acknowledgments. The authors thank Eric Slater, Lloyd Green, Michael Goldin, and Chris Neely for the design and construction of the CTD and sonar systems used in this effort, as well as their at-sea operation. Discussions with Bill Young and Mark Merrifield proved extremely helpful. This work was supported by the Office of Naval Research under Contract N00014-94-1-0046 and the National Science Foundation Grant OCE 91-10553.

APPENDIX

The Probability Density Function of Overturning

Suppose a realization of the Richardson number process takes the form of a vertical profile of Ri over L m depth. Regions of contiguous critical Ri are assumed to mix thoroughly, without subsequent entrainment. If in a given realization a single overturn of height Δ* is encountered, the probability of detection of critical Ri at scale Δ* per meter of water is just Δ*/L (Fig. 4a). This single overturn could also be thought of as two contiguous overturns of height Δ*/2 or n contiguous overturns of height Δ*/n. The probability of detection of an overturn of any scale less than Δ*, *per meter of depth*, is just Δ*/L.

Thus, defining

$$\hat{B}(\Delta) = \begin{cases} \Delta^*/L, & \Delta \le \Delta^* \\ 0, & \Delta > \Delta^*, \end{cases} \tag{A1}$$

we identify

$$\hat{B}(\Delta) = 1 - \hat{C}\,(4\ \mathrm{Ri}^*|\Delta), \tag{A2}$$

where $\hat{C}$ is the estimate of the cumulative distribution function of inverse Richardson number, evaluated for scale Δ at Ri = 1/4, R = 4 Ri* [Eq. (7a)].

From a second realization of the process we might see a second overturn of height Δ**, resulting in a $\hat{B}(\Delta)$, as given in Fig. 4b. Following many realizations, a smooth curve (Fig. 4c) will be approximated.

However, if one took the derivative of this curve with respect to Δ, a set of Dirac delta functions would result (Fig. 4d). We define

$$\hat{\hat{Q}}(\Delta) = -\frac{1}{\Delta}\frac{dB}{d\Delta}$$

(Fig. 4e) noting, $\int_{\Delta_0}^{\Delta_1}\hat{\hat{Q}}(\Delta)d\Delta$ gives the probability of seeing overturns of size Δ_0 through Δ_1 per meter of water per realization of the process.

REFERENCES

Anderson, S. A., 1992: Shear, strain, and thermohaline vertical fine structure in the upper ocean. Ph.D. thesis, University of California, San Diego, 173 pp.

Bretherton, F. P., 1969: Waves and turbulence in stably stratified fluids. *Radio Sci.,* **4,** 1279–1287.

Briscoe, M. G., 1977: Gaussianity of internal waves. *J. Geophys. Res.,* **82,** 2117–2126.

Cairns, J. L., and G. O. Williams, 1976: Internal wave observations from a midwater float. *J. Geophys. Res.,* **81,** 1943–1950.

Desaubies, Y., and W. K. Smith, 1982: Statistics of Richardson number and instability in oceanic internal waves. *J. Phys. Oceanogr.,* **12,** 1245–1259.

Duda, T. M., and C. S. Cox, 1989: Vertical wavenumber spectra of velocity and shear at small internal wave scales. *J. Geophys. Res.,* **94,** 939–950.

Evans, D. L., 1982: Observations of small-scale shear and density structure in the ocean. *Deep-Sea Res.,* **29,** 581–595.

Gargett, A. E., P. J. Hendricks, T. B. Sanford, T. R. Osborn, and A. J. Williams III, 1981: A composite spectrum of vertical shear in the upper ocean. *J. Phys. Oceanogr.,* **11,** 1258–1271.

Garrett, C. J. R., and W. H. Munk, 1972a: Space–time scales of internal waves. *Geophys. Fluid Dyn.,* **3,** 225–264.

——, and ——, 1972b: Ocean mixing by breaking internal waves. *Deep-Sea Res.,* **19,** 823–832.

——, and ——, 1975: Space–time scales of internal waves. A progress report. *J. Geophys. Res.,* **80,** 291–297.

Gregg, M. C., 1989: Scaling turbulent dissipation in the thermocline. *J. Geophys. Res.,* **94,** 9686–9698.

——, and E. Kunze, 1991: Shear and strain in Santa Monica basin. *J. Geophys. Res.,* **96,** 16 709–16 719.

——, H. E. Seim, and D. B. Percival, 1993: Statistics of shear and turbulent dissipation profiles in random internal wavefields. *J. Phys. Oceanogr.,* **23,** 1787–1799.

Henyey, F. S., J. Wright, and S. M. Flatte, 1986: Energy and action flow through the internal wave field: An eikonal approach. *J. Geophys. Res.,* **91,** 8487–8495.

Howard, L. N., 1961: Note on a paper of John W. Miles. *J. Fluid Mech.,* **10,** 509–512.

Miles, J. W., 1961: On the stability of heterogeneous shear flows. *J. Fluid Mech.,* **16,** 209–227.

Muller, P., E. A. D'Asaro, and G. Holloway, 1992: Internal gravity waves and mixing. *Dynamics of Oceanic Internal Gravity Waves,* SOEST Publications Series, University of Hawaii, 503 pp.

Munk, W. H., 1966: Abyssal recipes. *Deep-Sea Res.,* **13,** 707–730.

——, 1981: Internal waves and small scale processes. *Evolution of Physical Oceanography,* B. A. Warren and C. Wunsch, Eds., The MIT Press, 264–290.

Pinkel, R., and S. Anderson, 1992: Toward a statistical description of finescale strain in the thermocline. *J. Phys. Oceanogr.,* **22,** 773–795.

——, and ——, 1997: Shear, strain, and Richardson number variations in the thermocline. Part I: Statistical description. *J. Phys. Oceanogr.,* **27,** 264–281.

——, J. T. Sherman, J. A. Smith, and S. Anderson, 1991: Strain: Observations of the vertical gradient of isopycnal vertical displacement. *J. Phys. Oceanogr.,* **21,** 527–540.

Polzin, K. L., 1992: Observations of turbulence, internal waves, and background flows: An inquiry into the relationship between scales of motion. MIT/WHOI Report WHOI-92-39, Woods Hole Oceanographic Institution, 243 pp.